

Mid-Infrared Variations of R Coronae Borealis Stars

N. Kameswara Rao^{1,2}, & David L. Lambert²

¹*Indian Institute of Astrophysics, Bangalore 560034, India*

²*The W.J. McDonald Observatory and Department of Astronomy, The University of Texas at Austin, Austin, TX 78712-1083, USA*

Accepted Received ; in original form

ABSTRACT

Mid-infrared photometry of R Coronae Borealis stars obtained from various satellites from *IRAS* to *WISE* has been utilized in studying the variations of the circumstellar dust's contributions to the spectral energy distribution of these stars. The variation of the fractional coverage (R) of dust clouds and their blackbody temperatures (T_d) have been used in trying to understand the dust cloud evolution over the three decades spanned by the satellite observations. In particular, it is shown that a prediction $R \propto T_d^4$ developed in the paper is satisfied, especially by those stars for which a single collection of clouds dominates the IR fluxes.

Key words: Star: individual: R CrB: variables: circumstellar matter :other

1 INTRODUCTION

R Coronae Borealis stars (here, RCBs) are a rare class of peculiar variable stars. Currently known stars number about 68 in the Galaxy, 19 in Large Magellanic Cloud and three in the Small Magellanic Cloud (Clayton 2012). Two principal defining characteristics of RCBs are (i) a propensity to fade at unpredictable times by up to about 8 magnitudes as a result of clouds of soot intercepting the line of sight to the star, and (ii) a supergiant-like atmosphere that is very H-deficient and He and C-rich.

RCB stars manufacture and disperse soot from a formation site near the star (Loreta 1934, O'Keefe 1939). The soot particles absorb star light and reemit the energy in the infrared (e.g., Feast et al. 1997). Often, soot particles are sufficiently close to the star that they achieve an equilibrium temperature of several hundred degrees and so emit in the mid-infrared bands. Such emission is measured with difficulty from the ground. Fortunately, several Earth-orbiting satellites built for infrared photometric surveys have now reported measurements on RCBs. Available data are too sparse and inhomogeneous to define the variation of RCB dust emission on a daily, monthly or even annual timescale but mean properties of the infrared emission should be extractable to enable searches for correlations between dust shell properties derived from the infrared emission and other RCB properties such as chemical compositions.

The *Infrared Astronomical Satellite*, *IRAS* provided the first systematic photometry of these stars (Walker 1986; Rao & Nandy 1986) to complement limited ground-based photometry carried out earlier (e.g., Feast & Glass 1973; Kilkenny & Whittet 1984). *IRAS* confirmed not only that

warm (300–900K) dust was common around RCBs but also showed the presence of cold (i.e., distant from the star) dust for strong infrared emitting stars (Rao & Nandy 1986). *IRAS* was followed by the *Infrared Space Observatory*, *ISO*. Although *ISO* provided higher spectral resolution mid-infrared spectroscopy and SEDs, it observed only a few bright RCBs (Lambert et al. 2001). Clayton et al. (2011) recently discovered using the *Herschel* satellite that the cold dust shell around R CrB radiates up to at least a wavelength of 1000 μm .

Major progress in infrared photometry of RCBs could occur only after the launch of *Spitzer* satellite which provided high-quality low-resolution 8–40 μm spectra using IRS for a major sample of RCBs (García-Hernández et al. 2011, here Paper I). *Spitzer* spectra were combined with optical and near-infrared photometry at maximum light corrected for interstellar reddening to define a star's spectral energy distribution (SED) from which characteristics of the infrared emitting dust shell were extracted (García-Hernández et al. 2011, 2013). Recently, it was realised that mid-infrared band colours could distinguish RCB stars from other types of variable stars rather uniquely (Tisserand 2012; Miller et al. 2013; Tisserand et al. 2013).

Following *Spitzer*, the satellites *AKARI* and *WISE* have provided photometric surveys from which observations of RCBs may be extracted. The *AKARI* infrared camera surveyed the sky at 9 and 18 μm between 2006 May 6 and 2007 August 28 (Ishihara et al. 2010). A few RCBs were also detected by *AKARI* at 65, 90 and 160 μm . *WISE*'s survey was conducted at 3.0, 4.6, 12 and 22 μm in 2010 (Wright et al. 2010). Tisserand (2012) used the available *AKARI*, *WISE* and other photometry to investigate the infrared colours and

the spectral energy distributions from the optical to the mid-infrared and to characterize the circumstellar dust emission from a large sample of RCBs.

Here, we assemble and discuss the SEDs of our *Spitzer* sample and their dust emission as measured in the mid-infrared by the series of satellites from *IRAS* to *AKARI* and *WISE* and by published ground-based photometry.

2 SPECTRAL ENERGY DISTRIBUTIONS

In Paper I, *Spitzer* satellite spectra of RCBs in the wavelength range of 5 to 40 μm were paired with visual to near-infrared photometry of the star to obtain a comprehensive SED of the star. Observed fluxes were corrected for interstellar reddening. For details, please see Paper I. Comparisons were made with *IRAS* 10 and 25 μm fluxes and, where available with ground-based infrared photometry. Here, we complement these *Spitzer* and *IRAS* observations with *AKARI* (Ishihara et al. 2010) and *WISE* (Wright et al. 2010) satellite band fluxes (Table 1). *WISE* observations were done in four bands 3.0, 4.6, 12 and 22 microns whereas *AKARI* observations in the two bands at 9.0 and 18.0 microns have been used. The flux calibration adopted was from Wright et al. (2010) for *WISE* magnitudes and Ishihara et al. (2010) for *AKARI*. The epochs of these observations have been taken as 2006.0 and 2010.5 for *AKARI* and *WISE*, respectively. Epochs of the *Spitzer* observations are given in Paper I: a majority were taken in about mid-2008. To compare the flux densities of *Spitzer* spectra with the other satellites bands we choose the the same effective wavelengths of these bands 9, 12, 18 μm and obtained monochromatic flux densities from the *IRS* spectra. We made a linear fit to the data points of three wavelengths on either side of these chosen band wavelengths and obtained the flux density listed in Table 1 at these central wavelengths. These flux densities are not band averaged flux densities as given by other satellites. Flux density uncertainties were taken from the following sources: *IRAS* Point Source Catalogue 2.0 via SIMBAD; *AKARI* and *WISE* from <http://irsa.ipac.caltech.edu/cgi-bin/Gator/nph-query>; *Spitzer* from the noise in the observed spectra. For the *Spitzer* 9 μm flux density, the uncertainties are less than 0.01 Jy for all stars and are not indicated in Table 1. *WISE* measurements at 3.0 and 4.6 microns are not tabulated but are shown in the appropriate figures which follow. Except for the *IRAS* photometry, the ground-based and *AKARI* and *WISE* photometry have not been colour corrected. Apart from the 12 μm *WISE* band, the other bands are sufficiently narrow not to require a significant colour correction for these spectra which span a narrow (500 – 900 K) temperature range.

Earlier, Tisserand (2012) used *WISE* as well as *AKARI* magnitudes to construct SEDs of RCBs. The recent release of the *WISE* catalogue contains more and fainter RCBs than dealt with by him and the magnitudes also were revised (IPAC website <http://irsa.ipac.caltech.edu/cgi-bin/Gator/nph-query>). It was mentioned by Tisserand (2012) that 4.6 micron band *WISE* magnitudes less than 4.0 have saturation problems. Some of the bright RCBs like R CrB, RY Sgr etc. were too bright for accurate photometry. Table 1 gives the flux density measurements from the four satellites and, where available, ground-based mid-IR pho-

tometry. We make limited use of the *WISE* flux densities at 3.0 and 4.6 μm . These quantities are not tabulated in Table 1 but are provided by Tisserand (2012).

We have used the methodology described in Paper I for constructing the SED of the star and its dusty circumstellar shell. Interstellar reddening estimates listed in Paper I have been applied before constructing the SEDs; this correction for reddening primarily affects the stellar component of the combined SED. Blackbody fits have been made to the combined SEDs with the temperature of the stellar blackbody taken from Paper I.

The blackbody fits provide the dust temperature T_d and the fraction of the stellar energy radiated by the cool circumstellar shell $R = f_{cool}/f_{star}$ where f refers to the integrated flux density. In general, the dust component for RCBs can be well represented by a single blackbody. In a few cases, a second and cooler blackbody is added to provide an adequate fit to the IR fluxes. With a more detailed coverage of the near-IR energy distribution, it might be possible to include a blackbody to represent emission by warmer dust near the star. The *WISE* observations at 3.0 and 4.6 μm and ground-based L and M photometry sample warmer dust, if present. Our focus here is on the dust emitting at mid-IR wavelengths.

3 DISCUSSION - THE PUFF MODEL

3.1 The concept

Our discussion of SEDs is framed in terms of the random dust-puff model for dust formation and ejection. In this scenario (Feast 1979, 1986, 1996, 1997; Feast et al. 1997; Herbig 1949; Payne-Gaposchkin 1963; Clayton et al. 1992), dust is ejected from points on or near the RCB surface in the form of puffs or clouds which then are expelled away from the stellar surface. Only those puffs formed on or very close to the Earth-facing hemisphere of the RCB will result in the characteristic fading. All puffs but those eclipsed by the star will contribute to the infrared signal from the dust. In a given circumstellar envelope, there may be one, several or many puffs. Puffs may be created at preferred parts of the stellar surface or uniformly over the surface. The rate of creation of fresh puffs will likely vary from star to star. Those RCBs prone to frequent formation of puffs will be expected to have nearly time-independent R values. The amplitude of IR variations will depend on several factors such as the number of puffs and their mean contribution to the mid-IR flux: a star with many weak puffs is likely to show smaller variations than a star with a few strong puffs. On the other hand, RCBs producing puffs infrequently are likely to have smaller mean R values with larger variations resulting as a puff moves away from the star and subsequently a fresh puff is ejected. In this simple picture, puffs are formed and expand away from the star, i.e., there is no mechanism for storing dust (and gas) near the star as in a circumstellar disk. Chesneau et al. (2014) from interferometric observations of V854 Cen show that this star's dust is concentrated in an elongated structure which, as the authors note, may reflect a bipolar wind off the star. Quasi-stable dusty disks have been found as circumbinary features for some binary stars. It has yet to be shown that V854 Cen is a binary star.

Table 1. IRAS, AKARI, Spitzer, WISE flux densities (Jy) at selected wavelengths

Star	<i>IRAS</i> ^a 1983		<i>AKARI</i> 2006		Spitzer			<i>WISE</i> 2010.5	
	12 μ m	25 μ m	9 μ m ^b	18 μ m	9 μ m	12 μ m	18 μ m	12 μ m	22 μ m
XX Cam	0.23	0.14		1.39 \pm 0.06				1.21 \pm 0.02	0.61 \pm 0.01
SU Tau	9.50 \pm 0.76	4.14 \pm 0.29	14.72 \pm 0.50	6.16 \pm 0.05		7.52 \pm 0.08	4.88 \pm 0.06	7.12 \pm 0.07	3.35 \pm 0.04
UX Ant			0.10 \pm 0.01					0.08 \pm 0.00	0.04 \pm 0.00
UW Cen	7.81 \pm 0.47	5.57 \pm 0.33	9.76 \pm 0.07	5.70 \pm 0.05	9.78	7.66 \pm 0.07	5.29	7.36 \pm 0.05	4.67 \pm 0.05
Y Mus	0.83 \pm 0.07	0.29 \pm 0.03	0.23 \pm 0.02		0.18	0.18 \pm 0.01	0.14 \pm 0.01	0.13 \pm 0.00	0.12 \pm 0.00
DY Cen	1.05 \pm 0.06	0.84 \pm 0.07	0.54 \pm 0.02	0.89 \pm 0.02	0.50	0.87 ^c	1.07	0.66 \pm 0.01	0.91 \pm 0.01
V854 Cen	18.42 \pm 0.9	5.88 \pm 0.4	22.97 \pm 1.2	7.36 \pm 0.03	16.36	11.59 \pm 0.03	6.79 \pm 0.0	17.78 \pm 0.2	5.83 \pm 0.04
Z UMi	1.79 \pm 0.11	0.62 \pm 0.04	1.72 \pm 0.03	0.76 \pm 0.02	1.54	1.18 \pm 0.02	0.69 \pm 0.05	1.23 \pm 0.01	0.56 \pm 0.01
S Aps	2.71 \pm 0.11	1.02 \pm 0.07	1.97 \pm 0.02	1.00 \pm 0.02	3.14	2.30 \pm 0.02	1.31 \pm 0.04	0.91 \pm 0.01	0.60 \pm 0.01
R CrB	33.83 \pm 1.4	13.81 \pm 0.6	52.99 \pm 2.4	21.48 \pm 0.03		23.72 \pm 0.3	13.66 \pm 0.4	45.95 \pm 0.8	17.52 \pm 0.1
RT Nor	0.85 \pm 0.09	0.39 \pm 0.04	0.26 \pm 0.04	0.23 \pm 0.02	0.15	0.18 \pm 0.00	0.20 \pm 0.00	2.01 \pm 0.02	0.77 \pm 0.01
RZ Nor	3.08 \pm 0.09	1.77 \pm 0.09	3.12 \pm 0.26	1.70 \pm 0.08	3.63	2.93 \pm 0.01	2.01 \pm 0.01	2.05 \pm 0.03	1.26 \pm 0.02
V517 Oph	6.0 \pm 0.36	1.90 \pm 0.19	6.76 \pm 0.24			4.86 \pm 0.06	2.75 \pm 0.06	4.47 \pm 0.04	1.86 \pm 0.02
V2552 Oph								0.36 \pm 0.00	0.16 \pm 0.00
V532 Oph	0.52 \pm 0.04			0.47 \pm 0.06				0.60 \pm 0.01	0.30 \pm 0.01
V1783 Sgr	2.84 \pm 0.14	1.00 \pm 0.09	3.92 \pm 0.25	1.90 \pm 0.03	2.97	2.50 \pm 0.02	1.66 \pm 0.04	1.62 \pm 0.02	0.79 \pm 0.02
WX CrA	1.89 \pm 0.09	0.61 \pm 0.05	1.74 \pm 0.10	0.81 \pm 0.00	0.89	0.73 \pm 0.02	0.53 \pm 0.03	0.90 \pm 0.01	0.41 \pm 0.01
V739 Sgr	1.10 \pm 0.09	0.28 \pm 0.04	1.64 \pm 0.06	0.84 \pm 0.00	1.45	1.20 \pm 0.01	0.79 \pm 0.02	0.86 \pm 0.01	0.42 \pm 0.01
V3795Sgr	3.42 \pm 0.27	1.36 \pm 0.20	4.57 \pm 0.14	1.95 \pm 0.07	3.31	2.63 \pm 0.05	1.57 \pm 0.04	1.70 \pm 0.02	0.93 \pm 0.01
VZ Sgr	1.13 \pm 0.08	0.60 \pm		0.28 \pm 0.10	1.30	1.08 \pm 0.02	0.86 \pm 0.04	0.30 \pm 0.00	0.16 \pm 0.00
RS Tel	1.31 \pm 0.08	0.57 \pm 0.05	1.87 \pm 0.10	0.77 \pm 0.01	1.82	1.33 \pm 0.00	0.90 \pm 0.00	0.96 \pm 0.01	0.51 \pm 0.01
MACHO^d					0.54	0.45	0.32	0.27 \pm 0.00	0.17 \pm 0.00
GU Sgr	0.97 \pm 0.07	0.66 \pm 0.14	1.29 \pm 0.14	0.75 \pm 0.1				1.74 \pm 0.02	0.76 \pm 0.01
NSV11154	0.41 \pm 0.02	0.17 \pm 0.02	0.63 \pm 0.01	0.30 \pm 0.03				0.24 \pm 0.00	0.15 \pm 0.00
MV Sgr	0.86 \pm 0.19	1.48 \pm 0.13	0.33 \pm 0.02	1.01 \pm 0.01	0.32	0.56 \pm 0.01	1.06 \pm 0.03	0.38 \pm 0.01	1.06 \pm 0.02
FH Sct	0.54 \pm 0.05	0.40 \pm 0.05	1.40 \pm 0.03	0.66 \pm 0.05	1.02	0.92 \pm 0.01	0.68 \pm 0.02	1.06 \pm 0.01	0.52 \pm 0.01
V CrA	4.95 \pm 0.20	2.00 \pm 0.14	3.61 \pm 0.21	2.17 \pm 0.01	3.32	3.02 \pm 0.00	2.40 \pm 0.01	3.46 \pm 0.03	1.96 \pm 0.02
SV Sge	3.29 \pm 0.23	1.66 \pm 0.10	3.85 \pm 0.44	2.29 \pm 0.10	2.15	2.10 \pm 0.02	1.69 \pm 0.03	1.36 \pm 0.01	1.10 \pm 0.02
V1157 Sgr	2.63 \pm 0.21	0.89 \pm 0.08	2.57 \pm 0.00	1.14 \pm 0.02	2.29	1.74 \pm 0.02	1.08 \pm 0.03	1.64 \pm	0.79 \pm
RY Sgr	63.88 \pm 4.5	20.80 \pm 0.8	48.00 \pm 3.7	20.18 \pm 1.0		26.77 \pm 0.4	17.25 \pm 0.3	33.16 \pm 0.9	13.89 \pm 0.2
ES Aql	1.18 \pm 0.09	0.39 \pm 0.07	1.94 \pm 0.13	0.88 \pm 0.04	1.77	1.34 \pm 0.01	0.87 \pm 0.02	1.34 \pm 0.02	0.61 \pm 0.01
V482 Cyg	0.85 \pm 0.05	0.35 \pm 0.07	1.13 \pm 0.04	0.46 \pm 0.02	0.58	0.49 \pm 0.00	0.38 \pm 0.00	0.72 \pm 0.01	0.33 \pm 0.01
U Aqr	1.12 \pm 0.09		1.26 \pm 0.14	0.75 \pm 0.00	0.89	0.86 \pm 0.01	0.82 \pm 0.02	0.52 \pm 0.01	0.37 \pm 0.01
UV Cas	3.81 \pm 0.15	1.28 \pm 0.09	1.13 \pm 0.05	0.80 \pm 0.03	0.87	0.83 \pm 0.01	0.65 \pm 0.02	0.60 \pm 0.01	0.49 \pm 0.01

^a: Color corrected. Mainly from Walker (1986).

^b: Uncertainties are less than 0.01 Jy for all stars. ^c: Emission features exist at 12 μ m and 18 μ m in the *Spitzer* spectrum of DY Cen (García-Hernández et al. 2011, 2013). ^d: MACHO135.27132.51

Evidence for bipolar outflows have been presented earlier by Rao & Lambert (1993) for V854 Cen and Clayton et al. (1997) for R CrB.

Information about the formation and evolution of the circumstellar dust shell for RCBs is, thus, provided by the temporal evolution of the infrared flux in terms of its spectral distribution and intensity which here are crudely represented by the covering factor R and the blackbody temperature T_d . Unfortunately, available infrared measurements are extremely sparse because the observations are difficult to obtain; ground-based mid-IR photometry is a rarely practiced art and infrared-capable satellites are launched infrequently. An exceptional database is the SAAO series of JHKL photometry of bright southern RCBs (Feast et al. 1997). And, in particular, Bogdanov et al. (2010) mounted a beautiful long-term campaign of JHKLM observations of UV Cas.

3.2 Variability

Here, we compare mid-IR fluxes obtained with the satellites *IRAS*, *AKARI*, *Spitzer* and *WISE*. The epochs of these surveys are 1983 for *IRAS*, 2006 for *AKARI*, 2005-2008 for *Spitzer* and 2010 for *WISE*. Long-term – two decades approximately – variations are estimated from comparison between *IRAS* and the other three surveys. Shorter term – one to a few years – variations are estimated by comparisons among the fluxes from the three most recent satellites. Our present comparisons are an extension of the *IRAS* – *Spitzer* comparison discussed in Paper I where the *Spitzer* 12 and 25 μ m fluxes for a large RCB sample were compared with their *IRAS* counterparts obtained about 25 years previously.

IRAS and *Spitzer* 12 μ m flux densities are compared in Figure 1. When a few outliers are excluded, the mean re-

Table 2. Dust Parameters from MidIR SEDs of RCBs at various epochs.

Star	Ground/Other			<i>IRAS</i> 1983		<i>AKARI</i> 2006		Spitzer			<i>WISE</i> 2010.5		Mean R
	Epoch	R	T _d	R	T _d	R	T _d	Epoch	R	T _d	R	T _d	R _{av}
XX Cam				≤0.01	500	0.02	550				0.01	650	0.01±0.01
SU Tau				0.46	600	0.99	850	2008.4	0.44	635	0.54	750	0.61±0.23
UX Ant						0.14	650				0.14	650	0.14
UW Cen	1984 ^e	0.35	620	0.44	630	0.44	600	2008.7	0.44	636	0.44	650	0.38±0.10
Y Mus	1984 ^b	0.14	980	0.08	655	0.01	420	2008.4	0.01	395	0.01	340	0.06±0.06
V854 Cen	1996.8 ^a	0.94	1100	0.57	920	0.54	900	2007.8	0.30	900	0.54	880	0.58±0.22
Z UMi				0.95	850	0.79	900	2008.9	0.41	695	0.79	900	0.74±0.20
S Aps				0.42	750	0.22	710	2008.4	0.37	730	0.14	950	0.29±0.11
R CrB	1998.0 ^g	0.30	810	0.20	680	0.30	810	2004.6	0.30	950	0.30	810	0.28±0.04
RT Nor	1984 ^b	0.11	920	0.08	500	0.02	400	2005.4	0.01	365	0.46	850	0.14±0.17
RZ Nor	1983.4 ^c	0.72	720	0.72	720	0.54	650	2006.3	0.64	640	0.37	610	0.57±0.13
V517 Oph				0.98	850	0.92	885	2008.4	0.92	885	0.83	880	0.91±0.05
V2552 Oph											0.09	800	0.09
V532 Oph^f				0.03	400						0.07	720	0.05±0.02
V1783 Sgr				0.53	770	0.65	790	2008.4	0.27	554	0.24	670	0.42±0.17
WX CrA				0.46	670	0.39	740	2008.9	0.14	570	0.35	870	0.33±0.12
V739 Sgr				0.98	900	0.71	700	2008.4	0.57	656	0.68	850	0.74±0.15
V3795 Sgr				0.50	700	0.36	650	2008.4	0.29	600	0.17	580	0.33±0.12
VZ Sgr				0.21	700	0.11	780	2008.4	0.21	692	0.07	770	0.15±0.06
RS Tel	1984 ^b	0.26	790	0.28	700	0.36	850	2005.78	0.33	830	0.15	650	0.28±0.07
MACHO135.27132.51													
GU Sgr	1977.6 ^d	0.45	910	0.06	400	0.12	600				0.45	910	0.27±0.18
NSV 11154				0.63	720	0.92	800				0.40	750	0.65±0.21
FH Sct				0.04	393	0.17	740	2008.5	0.10	537	0.25	940	0.14±0.09
V CrA	1984 ^b	0.69	640	0.87	670	0.45	580	2005.4	0.38	550	0.65	700	0.61±0.18
SV Sge				0.17	730	0.11	600	2008.5	0.05	500	0.03	500	0.09±0.05
V1157 Sgr				0.89	880	0.60	820	2008.5	0.44	753	0.34	680	0.57±0.21
RY Sgr	1997.3 ^h	0.38	820	0.76	870	0.38	820	2004.89	0.20	675	0.38	820	0.42±0.18
ES Aql				0.70	830	0.70	830	2008.5	0.58	750	0.70	830	0.67±0.06
V482 Cyg				0.09	650	0.14	850	2004.96	0.04	580	0.20	970	0.12±0.06
U Aqr				0.37	560	0.37	560	2008.6	0.25	473	0.24	680	0.31±0.06
UV Cas				0.26	830	0.03	507	2008.5	0.03	507	0.02	510	0.08±0.10

^a V854 Cen was observed by *ISO* on 1996 September (Lambert et al. 2001). The R and T_d values refer to *ISO* observations. The *AKARI* and *WISE* photometry needed a combination of two black bodies to match the SED.

^b The ground based observations come from Kilkenny & Whittet (1984). Their observations were obtained mainly in April 1983.

^c The KW's and *IRAS* observation together defined the SED from which R and T_d has been estimated.

^d The ground based observations are from Glass (1978).

^e Goldsmith et al. (1987) also observed the star on 1985.5 from which R and T_d of 0.16 and 540K have been derived. They have been included in the average.

^f Both *IRAS* 12μm and *AKARI* 18μm fluxes together defined a black body SED for the R and T_d estimate.

^g R CrB was observed by *ISO* on 1998 January 15. The *ISO* SED could be fit by a combination of blackbodies 810 K, 750K and 550K. The flux densities from *AKARI* and *WISE* match very well the *ISO* spectrum. All three observations have same value of R.

^h RY Sgr was observed by *ISO* on 1997 March 25. The *ISO* spectrum could be fit with a single black body of 870K. The flux densities obtained with *AKARI* and *WISE* match the *ISO* spectrum very well. All three observations result in same R.

lation $F(IRAS) = 1.24F(Spitzer)$ provides a good fit to the data points and this linear relation is shown in the figure. A systematic offset of 24 per cent between *Spitzer* and *IRAS* observations may be due to the broad-band nature of the *IRAS* photometry and an imperfect color correction. Given that there is a roughly 10 per cent uncertainty affecting *IRAS* photometry, it would appear that many RCBs had similar 12 μm flux densities in 1983 and 2005-2008 but this is not to suggest that they did not vary in the nearly 30 year interval. Outliers include RY Sgr, V854 Cen, UV Cas, Y Mus, RT Nor and WX CrA with an exceptionally large ra-

tio of *IRAS* to *Spitzer* fluxes and FH Sct with an apparently small ratio of *IRAS* to *Spitzer* fluxes. The three stars – UV Cas, Y Mus, and RT Nor – showed a factor of five greater *IRAS* 12 μm flux than recorded by *Spitzer*. A striking and expected characteristic of the trio is that their covering factors R as obtained from *Spitzer* were very small (0.01 to 0.03) and among the lowest of the sample. For their *IRAS* fluxes, the R values were 0.07 – 0.28. In the puff model, the trio are most likely examples where very few puffs inhabit the circumstellar environment at any given time because ejection of fresh puffs is an infrequent event. Other outliers –RY

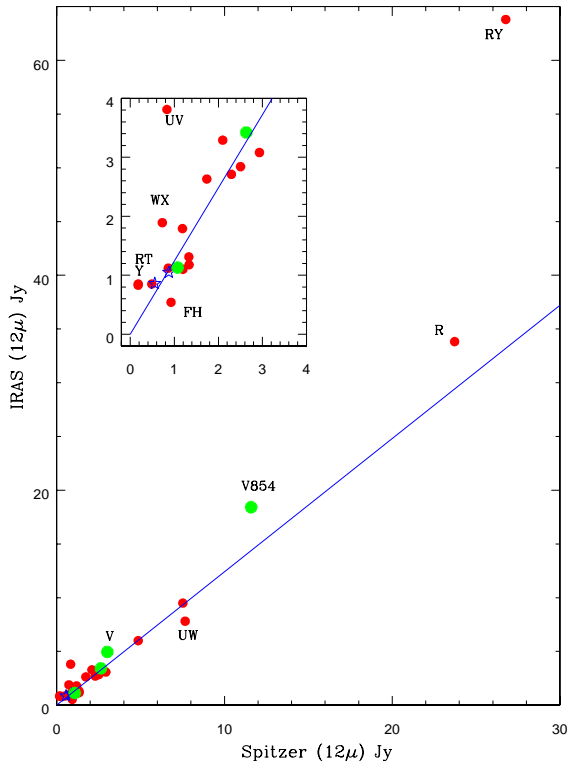


Figure 1. Flux densities F at $12\mu\text{m}$ from *Spitzer* versus the values from *IRAS*. The solid line shows the mean relation $F(\text{IRAS}) = 1.24F(\text{Spitzer})$ defined by the bulk of the sample. Outliers are identified by shorthand labels: RY Sgr, V854 Cen, UV Cas, WX CrA, Y Mus, RT Nor and FH Sct. Red points refer to majority RCBs as defined by Lambert & Rao (1994), the green points refer to minority RCBs and two blue stars refer to two hot RCBs (DY Cen and MV Sgr) given in Table 1.

Sgr, V854 Cen and WX CrA – show a less extreme difference between *IRAS* and *Spitzer* fluxes. This trio have larger R covering factors but would appear to be still affected by a change in the dust in their circumstellar shell. FH Sct, another low R star, is the only star in the sample which was fainter when observed by *IRAS* than by *Spitzer*.

A comparison of *Spitzer* and *AKARI* flux densities at $9\mu\text{m}$ is shown in Figure 2 where the relation $F(\text{AKARI}) = F(\text{Spitzer})$ is plotted. Similarly, *WISE* and *Spitzer* $12\mu\text{m}$ fluxes are compared in Figure 3 where the line corresponds to $F(\text{WISE}) = F(\text{Spitzer})$. In both figures, a few outliers are marked. In Figure 3, RT Nor is the outstanding outlier with its *WISE* flux density raised by a fresh ejection of dust. V854 Cen is again brighter than expected from its *Spitzer* flux density and the mean for the sample. Two stars – VZ Sgr and S Aps – have faded noticeably between their observations by *Spitzer* and then by *WISE*. An overall impression from these comparisons is that the mid-IR fluxes of the majority of the sampled RCBs are not subject to major variations over the 1 to 25 year timeframe.

Qualitatively, the three extreme outliers in Figure 1 – UV Cas, Y Mus and RT Nor – with the small R -values from *Spitzer* may be identified as stars which at the time of the *Spitzer* observations had little warm dust – few dust puffs

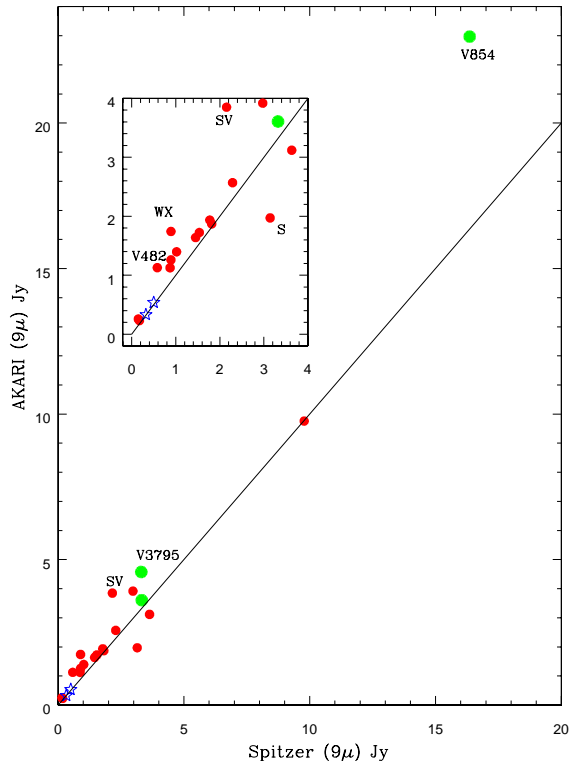


Figure 2. Flux densities F at $9\mu\text{m}$ from *Spitzer* versus the values from *AKARI*. The line shows the relation $F(\text{AKARI}) = F(\text{Spitzer})$. Distinct outliers are identified by shorthand labels: WX CrA, V482 Cyg, SV Sge, V854 Cen and S Aps. Note that there is no systematic shift between *AKARI* and *Spitzer* flux densities. The symbols are same as in Figure 1.

– in their circumstellar envelopes and, thus, large fractional changes in their mid-IR fluxes surely reflect fresh ejection of dust into the envelope and possibly a single ejection on or off the line of sight. We begin comparison of the SEDs constructed from *IRAS*, *Spitzer* and *AKARI*, and *WISE* observations with these three *IRAS* – *Spitzer* outliers – see Figure 4 for UV Cas, Figure 5 for Y Mus and Figure 6 for RT Nor.

For UV Cas, a valuable series of *JHKLM* photometry by Bogdanov et al. (2010) from 1984 (just following the *IRAS* observations) to 2009 (just following the *Spitzer* observations) suggests that a major episode of dust ejection occurred prior to the *IRAS* observations. This ejection did not cause a fading of the star. Following the ejection, UV Cas’s mid-IR flux decayed for about 2000 days with only two minor flux increases prior to 2009. Thus, the dust detected by *AKARI*, *Spitzer* and *WISE* was likely from the pre-*IRAS* ejection which had expanded away from the star in the intervening 25 years; the drop in dust temperature from 800 K to 510 K is consistent with this idea (Paper I). The dates of the *AKARI* and *WISE* observations generally bracket the *Spitzer* observations. Thus, it is not unexpected that for UV Cas that mid-IR fluxes from the three satellites are similar: Figure 4 shows that the *AKARI* and *Spitzer* fluxes are essentially identical but the *WISE* fluxes are lower suggesting that the expansion of the ‘1980’ dust ejection appears to

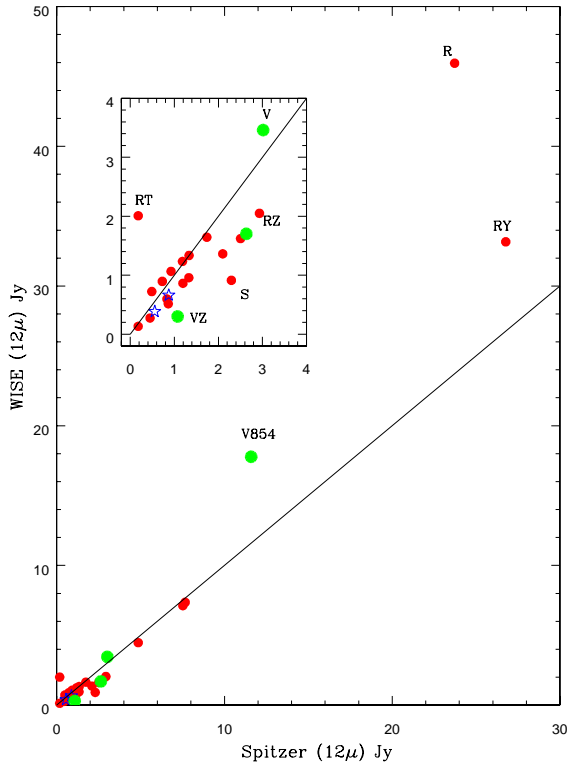


Figure 3. Flux densities F at $12\mu\text{m}$ from *Spitzer* versus the values from *WISE*. The solid line shows the mean relation $F(\text{WISE}) = F(\text{Spitzer})$ defined by the bulk of the sample. Distinct outliers are identified by shorthand labels: notably RT Nor, VZ Sgr, R CrB and S Aps. Symbols are as in Figure 1.

have continued and may have accelerated. A more quantitative discussion of the series of flux density measurements is given below in Section 3.3. However, Clayton et al. (2013) suggest that there might be some evidence for hundreds of km/s dust motions in the star.

IRAS to *WISE* photometry shows that Y Mus behaved similarly to UV Cas (Figure 5): the *IRAS* fluxes and the N flux from Kilkenny & Whittet (1984) are much greater than the fluxes from *AKARI*, *Spitzer* and *WISE*. Kilkenny & Whittet’s M and N observations were made in 1983 April during the year-long *IRAS* mission. Thus, the agreement between their N flux and the *IRAS* $10\mu\text{m}$ flux is expected in the absence of rapid changes of the IR flux (see discussion of RT Nor below). Unfortunately, there is no long-term series of mid-IR photometry comparable to Bogdanov et al.’s (2010) observations of UV Cas but we presume that the dust detected by *IRAS* moved away from Y Mus and had cooled substantially when detected by the other satellites. *AAVSO* records show Y Mus has not experienced a fading over the duration of the records (i.e., since early 1982) but these records do not sense puffs ejected off the line of sight to the star.

In two respects, different circumstances are found for RT Nor (Figure 6). The *AKARI* and *Spitzer* mid-IR fluxes of RT Nor are in good agreement but the *WISE* fluxes are about an order of magnitude stronger and about twice the *IRAS* fluxes. The inference is that a fresh ejection of dust

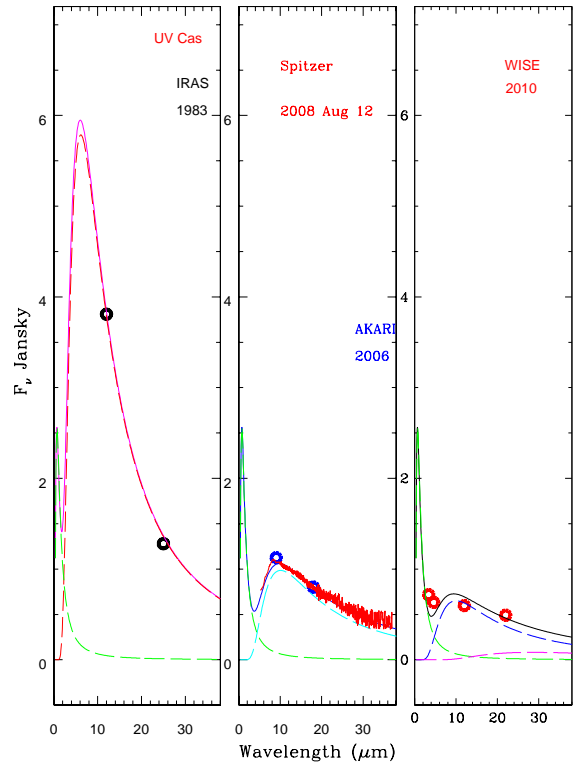


Figure 4. The SED for UV Cas from three sets of infrared observations: left panel - *IRAS*; middle panel - *AKARI* and *Spitzer*; right panel - *WISE*. In each panel, a two or three black body fit is shown with a 7200K black body (green dashed curve) representing the stellar fluxes corrected for interstellar reddening and much cooler blackbodies representing the dust emission (830K for *IRAS*, 507K and 180K for *AKARI* and *Spitzer* and 510K and 180K for *WISE*).

occurred after the 2005–2006 observations by *Spitzer* and *AKARI* and prior to the observation in 2010 by *WISE*. This sharp increase in mid-IR fluxes may be linked to a fading of the star: *AAVSO* records show that a minimum occurred between October 2008 when the star was at maximum and the next observation in mid-2009 when it was about five magnitudes below maximum, the first decline since 1990. A second aspect setting RT Nor apart from Y Mus is that Kilkenny & Whittet’s (1984) M flux is considerably less than the *IRAS* measurement even though the M measurement was made during the year-long *IRAS* mission. We conjecture that between the M and *IRAS* observations fresh dust was added to the circumstellar shell. The *AAVSO* observations show no dimming in this period so that dust replenishment must have occurred off the line of sight to the star. These few observations suggest that RT Nor is more active than either UV Cas or Y Mus.

Frequency of ejection of dust is likely related in some way to the occurrence of visual fadings characteristic of RCBs but, as the examples of UV Cas and Y Mus illustrate, not every ejection of dust results in a dimming of the star. Jurcsik (1996) estimated inter-fade intervals for RCBs from reported visual magnitudes. Her two longest intervals were for Y Mus (15300 days) and UV Cas (25500 days) with

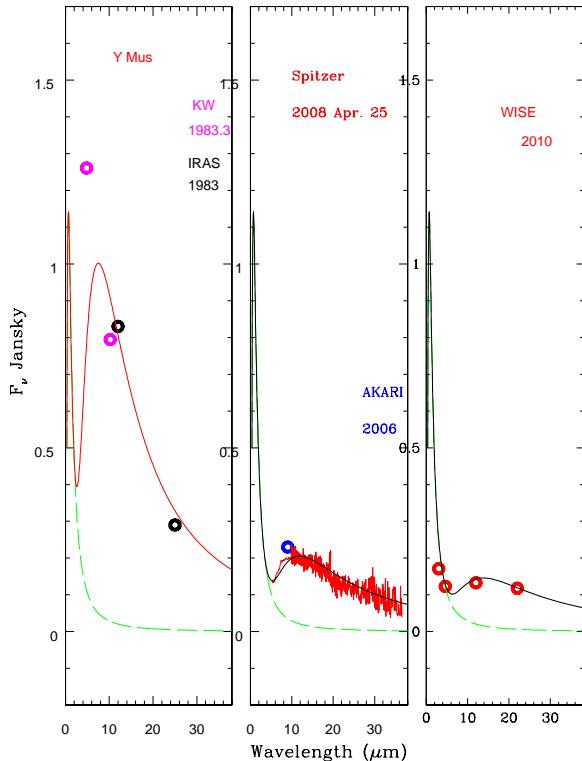


Figure 5. The SED for Y Mus from IR observations at different epochs: left-panel - *IRAS* with M and N fluxes from Kilkenny & Whittet (1984); middle panel - *AKARI* and *Spitzer*; right panel - *WISE*. In each panel, a two black body fit is shown with a 7200K black body (green dashed curve) representing the stellar fluxes corrected for interstellar reddening and a cooler black body representing dust emission (655K for *IRAS*, 420K for *AKARI* and 395K for *Spitzer*, and 340K for *WISE*).

typical values of 1000-2000 days reported for many RCBs. Thus, the low R values, the large amplitude mid-IR flux variations, and the long inter-fade intervals are all consistent with the view that UV Cas and Y Mus are presently poor producers of dust. Jurcsik's inter-fade interval for RT Nor is listed as 1950 days. In Paper I, we noted that the last minimum of RT Nor occurred about 15 years before 2008 and intimated that this suggested that Jurcsik's 1950 day estimate was an underestimate. However, recently two minima have been observed with onsets in about January 2009 and February 2013. One may conjecture, as noted above, that the January 2009 fading was responsible for the large increase in mid-IR flux between the *AKARI*–*Spitzer* and *WISE* observations.

At the opposite end of the range of factors R to the above trio of outliers are RCBs with large R . Among this sample, there is a range of variation in the mid-IR fluxes from the four satellites. At one extreme is ES Aql (Figure 7) where the mid-IR fluxes are very similar from all four satellites. The mean R is 0.67 ± 0.06 . As noted in Paper I, the cool RCB ES Aql declines frequently with a major decline about every year. Unless these optical declines reflect a preferred plane for puff ejection, ES Aql's circumstellar shell will be refreshed more frequently than once a year.

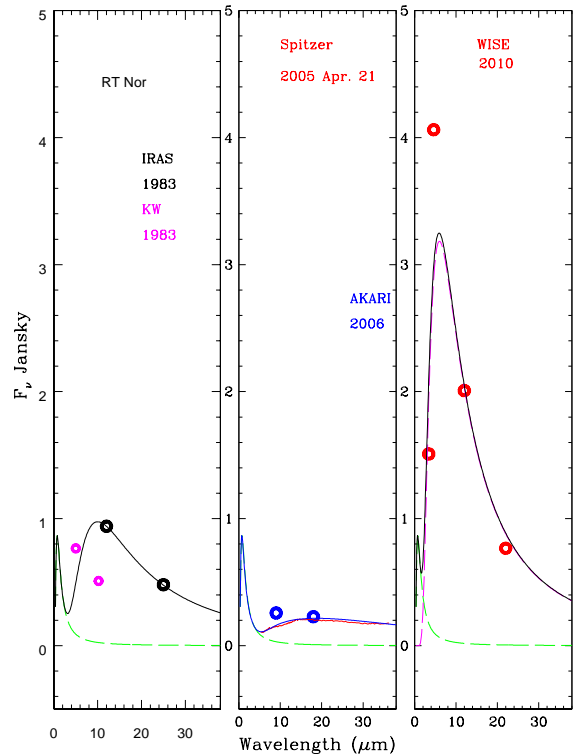


Figure 6. The SED for RT Nor from IR observations at different epochs: left-panel - *IRAS* with M and N fluxes from Kilkenny & Whittet (1984); middle panel - *AKARI* and *Spitzer*; right panel - *WISE*. In each panel, a two black body fit is shown with a 6700K black body representing the stellar fluxes corrected for interstellar reddening and a cooler black body representing dust emission (500K for *IRAS*, 400K for *AKARI*, and 850K for *WISE*).

Thus, ES Aql is likely an example where the shell hosts many puffs and conditions in the shell are essentially time invariant. A similar case may be the very active cool star V517 Oph which shows an average R of 0.91 ± 0.05 .

Other stars show modest variations in their mid-IR fluxes. One such example is SU Tau (Figure 8) where the shape of the mid-IR spectrum is very similar from epoch to epoch but the flux level varies by about 20-30%. SU Tau is a star which is frequently in decline: it 'has been three or more magnitudes below maximum light for nearly half of the last 20 years' (Paper I). With frequent known ejections of dust and quite possibly other ejections not causing fadings, it is not surprising that the shape of the mid-IR spectrum is almost invariant with modest changes in strength. In the language of the puff model, SU Tau may resemble ES Aql but have fewer puffs in its circumstellar shell such that a variation of one or two in the number of puffs emitting mid-IR radiation affects the total emitted flux.

V3795 Sgr is a star for which *IRAS*, *Spitzer* and *AKARI* give very similar mid-IR fluxes but *WISE* found appreciably lower fluxes (Figure 9). V3795 Sgr, a minority RCB (Lambert & Rao 1994), has experienced just two declines in the last 20 years and during the period of the *AKARI*–*WISE* observations was in recovery from one of those declines. A speculation is that the high speed wind seen during a recov-

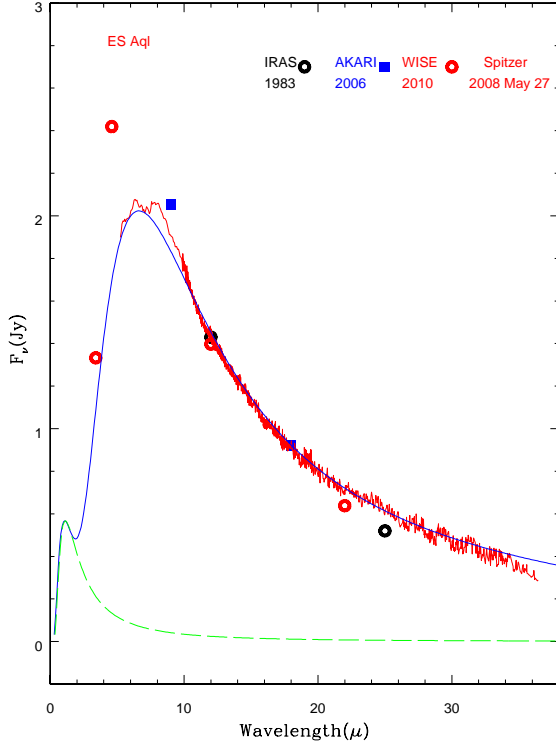


Figure 7. SED of ES Aql. The fit of two cool blackbodies (750K and 140K) is made to the *Spitzer* spectrum. *IRAS*, *AKARI* and *WISE* observations show no sensible departures from the *Spitzer* spectrum except that the *WISE* flux density at $6\mu\text{m}$ exceeds the expectation from the *Spitzer* spectrum. The stellar blackbody corresponding to a temperature of 4500 K is shown by the green dashed curve.

ery was responsible for sweeping a lot of dust outwards and, thus, to cooler temperatures (Rao et al. 1999; Clayton et al. 2013).

In the comparison with the *Spitzer* spectra obtained between the times of the *AKARI* and *WISE* observations, VZ Sgr (Figure 10), a minority RCB, stands out; both the *AKARI* and the *WISE* fluxes are about a factor of two to three less than the *Spitzer* and *IRAS* fluxes. At the time of the *Spitzer* observation and as noted in Paper I, VZ Sgr was in a deep minimum and several magnitudes below maximum light, but, at the time of the *AKARI* and *WISE* observations, the star was at maximum light. The high mid-IR flux seen by *Spitzer* is likely attributable to the fresh dust contributed by the on-going minimum but, in contrast to many other RCBs, the dust dispersed quickly; a high speed wind, as in V3795 Sgr, drove dust out to great distances?. One may conjecture that in cases such as V3795 Sgr and VZ Sgr puffs form and/or dissipate on timescales of a couple of years or less. This behaviour is in contrast to UV Cas, Y Mus and RT Nor where the timescale appears to be a couple of decades.

3.3 The run of R with T_d

Simple implementations of the puff model suggest a correlation between the covering factor R and the blackbody dust

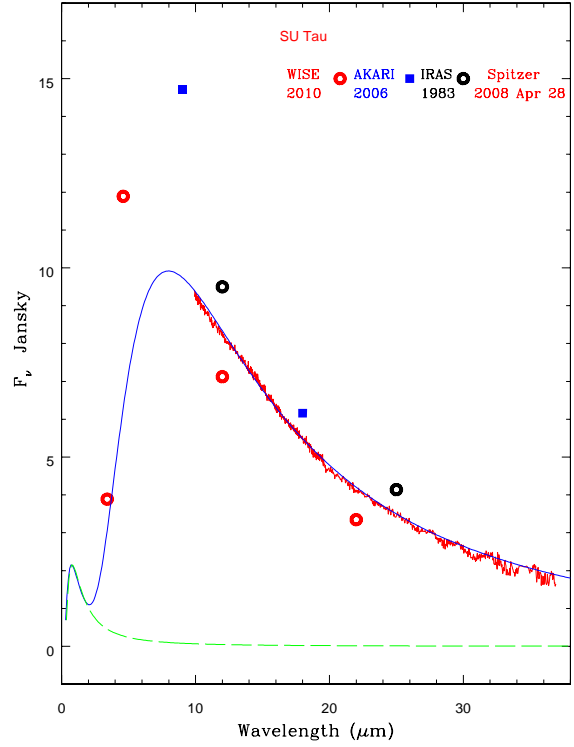


Figure 8. SED of SU Tau. The fit of a blackbody at 635K is made to the *Spitzer* spectrum. *IRAS*, *AKARI* and *WISE* observations show modest variations around the *Spitzer* spectrum with larger variations according to *AKARI* and *WISE* at shorter wavelengths. The stellar blackbody for 6500 K is shown by the green dashed curve.

temperature T_d . The factor R is defined to be the ratio of integrated dust emission to the stellar flux: $R = f_{\text{dust}}/f_{\text{star}}$ where corrections are applied for interstellar reddening. Consider the following scenario. Suppose that puffs occupy a volume $V(r)$ at a distance r from the central star and the dust in the puffs is at an equilibrium temperature T_d . The thickness of a puff is assumed to be small relative to the radial distance r . The integrated emission from the dust will be proportional to the product of $V(r)$ and T_d^4 . The dust temperature T_d is taken to be the equilibrium temperature of a grey dust grain in an optically thin puff*, i.e., $T_d \propto r^{-0.5}$ (Kwok 2007, p.314, Equation 10.32). In this simple picture, the ratio of star's integrated dust emission from a given set of puffs moving out from distance r_1 to r_2 is $f(r_1)/f(r_2) = V(r_1)/V(r_2) \times (T_d(r_1)/T_d(r_2))^4$. Thus, if the puffs are optically thin at IR wavelengths and their dust content are not evolving, f_{dust} is expected to scale with T_d^4 . Note that T_d is determined from the wavelength-dependence of the IR emission and f_{dust} from the integrated IR emission and, thus, T_d and f_{dust} are different measures of the IR emission.

* The ratio of absorption coefficients for carbonaceous grains at 5000\AA to $20\mu\text{m}$ is about a factor of 50 (Colangeli et al. 1995) and, thus, all but the clouds causing the very deepest of declines will be optically thin at mid-IR wavelengths.

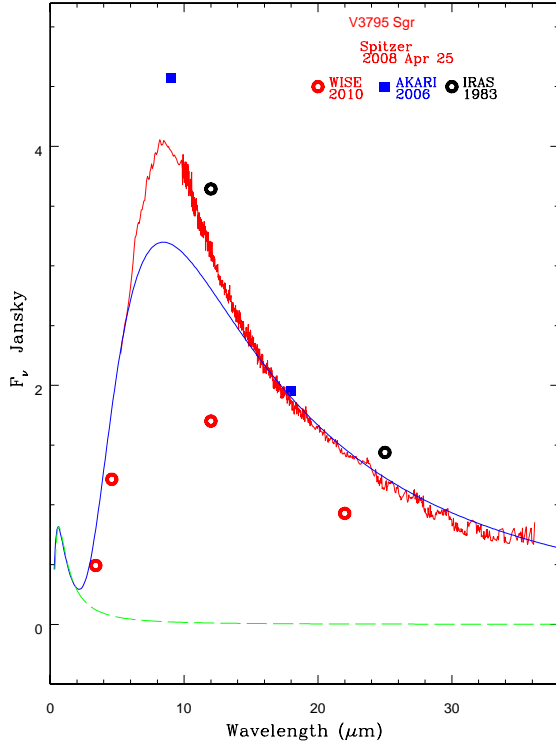


Figure 9. SED of V3795 Sgr. The fit of a blackbody at 600K is made to the *Spitzer* spectrum. *IRAS* and *AKARI* flux densities are similar to the *Spitzer* spectrum but the *WISE* observations show considerably lower fluxes with little change in the fitted blackbody temperature (580K versus 600K). The stellar blackbody of 8000 K is shown by the green dashed curve.

For the sample of RCBs, one expects that for a given T_d , there will be a spread in f_{dust} because the size and number of puffs and their distribution with radial distance r will vary from star to star and time to time for a particular star. The temperature T_d distance r relation will depend also on the stellar temperature T_* : $T_d \propto T_*$ – see Kwok above. Unfortunately, there is no observational way to determine the mean radial distance of the puffs at a given time or the distance travelled by puffs between two observations without assuming any expansion velocity for the dust. The covering factor $R = f_{dust}/f_{star}$ involves the stellar flux which is set by the luminosity L or the product $R_{star}^2 T_{star}^4$.

Observational pursuit of the above idea may be most instructive when applied to those stars in Table 2 for which R and T_d both decrease with time. In such cases, the reasonable inference is that a set of puffs is expanding away from their formation site near the star and, thus, experiencing cooling as observations proceeded from *IRAS* to *WISE*. Six stars (Y Mus, UV Cas, V3795 Sgr, SV Sge, V1157 Sgr and RT Nor) meet our condition with an additional four satisfying the condition but for an increase in R and T_d with the observation by *WISE* which we interpret as the signal of the formation of a new puff or cloud of puffs. In Figure 11, we show the R versus T_d relations for seven of the ten stars and also for V854 Cen, a star with a near-constant R and T_d . An evolutionary trend is indicated for each star. Note that

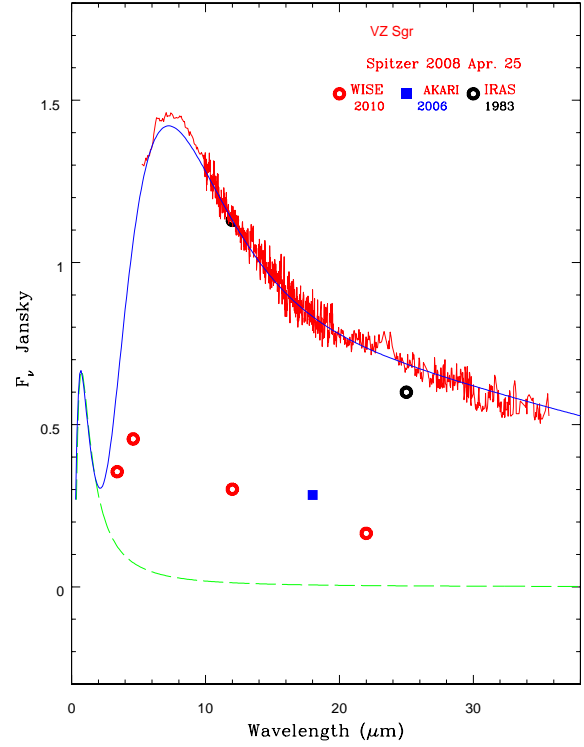


Figure 10. SED of VZ Sgr. The fit of a 690K blackbody is made to the *Spitzer* spectrum. *IRAS* flux densities fits this spectrum very well but the *AKARI* and *WISE* measurements are factors of three to four lower. The stellar blackbody of 7000 K is shown by the green dashed curve.

for RT Nor and V CrA, the *WISE* result is disconnected from the indicated trend from earlier photometry because, we suppose, fresh puffs have appeared between the time of the *Spitzer* and *WISE* observations. Inspection of Figure 11 shows that the evolutionary trends comprise a very diverse set. This diversity is likely to reflect several factors including the variation from star to star of the dust content, the different stellar luminosities and temperatures across the sample. RCBs may evolve at approximately constant luminosity but with a finite luminosity range across the sample. Stellar temperatures (see Paper I) for the stars represented by Figure 11 run from 4200 K for V1157 Sgr and SV Sge to 8000 K for V3795 Sgr.

If the simple model leading to the prediction that $f_{dust} \propto T_d^4$ for a given star is applicable, the diversity exhibited in Figure 11 will be markedly reduced when data for the sample are displayed after scaling such that $R/R(IRAS)$ is plotted versus $T_d/T_d(IRAS)$, as in Figure 12. Moreover, the model predicts that the scaled R and T_d should be related by $R \propto T_d^4$. This prediction shown in Figure 12 is a fine fit to the observational results.

When the other RCBs are added to Figure 12, they generally confirm the predicted trend but with increased scatter which may be attributed to their cloud of puffs is changing over the time period covered by the observations. The fact that the majority of RCBs satisfy the predicted relation suggests that the evolution of puffs around follows

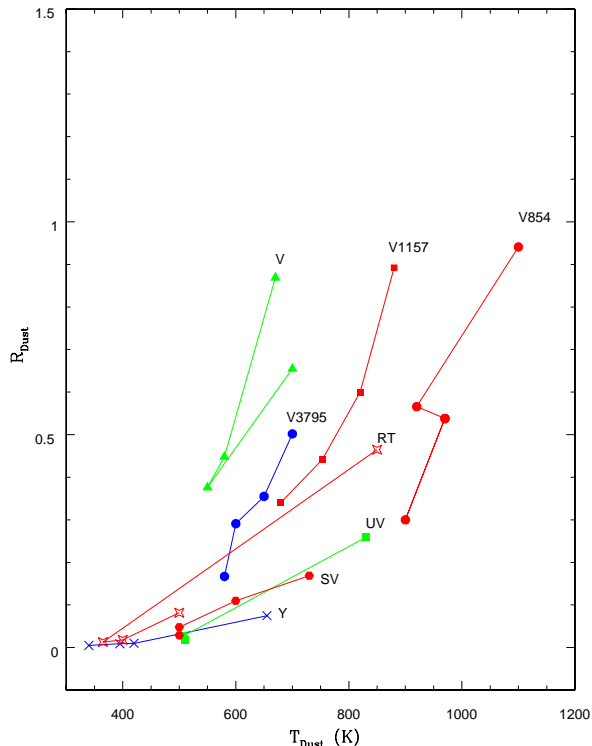


Figure 11. Variation of T_d with R for the sample of eight stars identified by the key on the figure. With the exception of V854 Cen, the chosen stars show a decline in T_d and R from *IRAS* to *WISE* with two – V CrA and RT Nor – showing an increase in mid-IR flux with the *WISE* observation.

a fairly common pattern. In three cases – RT Nor, GU Sgr and FH Sct – the R value and T_d relative to their *IRAS* values exceed unity suggesting that puffs have formed close to the RCB star. These observations fall between the R vs T_d^4 and T_d^2 relations.

As pointed in Paper I, it is very puzzling that the *IRAS* flux densities (Table 1) and now the R values (Table 2) are almost without exception greater than all observations since 1983. The implication is that almost all RCBs were at their infrared brightest in 1983 when observed by *IRAS*. Two speculations of this surprising result suggest themselves in isolation or in cooperation: (i) there is a systematic difference between the determination of the parameters R and T_d from the *IRAS* 12 and 25 μm flux densities and the three other satellites sources, and (ii) the dust shells (or, perhaps, the central stars) have evolved systematically over the thirty year interval since the *IRAS* observations. An explanation intrinsic to the RCBs is inconceivable. (point ii). It implies that the 1983 epoch was somehow a critical time of high R and high T_d for essentially each of the RCBs in our sample. This is most unlikely given that the RCB phase lasts several thousand years (Iben 1991).

3.4 Dust and Photospheric Composition

Photospheric composition should be one of the key variables influencing the formation of the carbon soot, a presumed

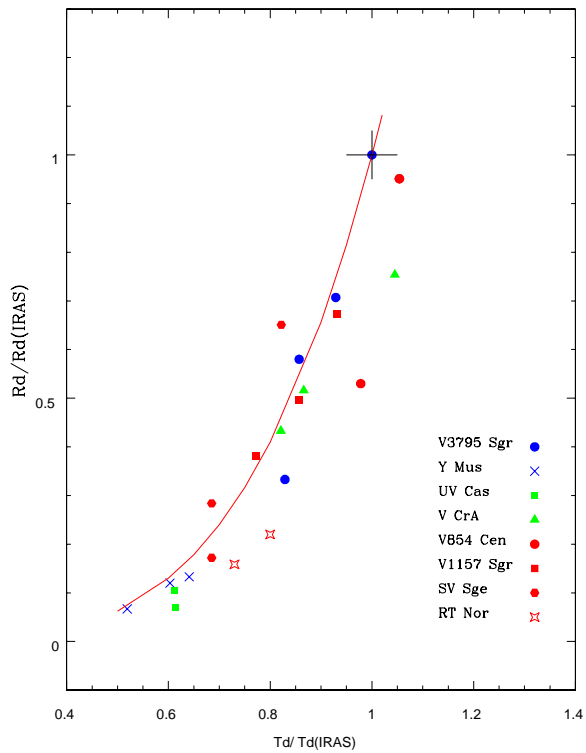


Figure 12. Normalized dust temperatures $T_d/T_d(\text{IRAS})$ and normalized covering factors $R/R(\text{IRAS})$. Points given for the eight stars represented in Figure 11 fit the predicted relation discussed in the text.

principal component of a puff’s dust. Chemical compositions of warm RCBs come mainly from Asplund et al. (2000) with results for V854 Cen from Asplund et al. (1998), V532 Oph from Rao et al. (2014) and V2552 Oph from Rao & Lambert (2003). Two introductory points about these compositions. First, the analysis by Asplund et al. (2000) using modern H-poor He-rich model atmospheres (Asplund et al. 1997) revealed what was termed ‘the carbon problem’, i.e., the C abundance returned from the analysis of a spectrum was about 0.6 dex less than the C abundance adopted in the model atmosphere’s construction. This problem was discussed by Asplund et al. (2000) who suggested that an abundance ratio was most likely more reliable than the abundance of either element. Second, Lambert & Rao (1994) in their abundance analysis, a precursor of that reported by Asplund et al. (2000), noted that the warm RCBs could be divided by composition into a ‘majority’ and ‘minority’ group. The minority RCBs differed from the majority principally in having a lower Fe and higher Si abundance and, hence, an extraordinary Si/Fe ratio, a ratio far in excess of that seen in any other major class of star such as metal-poor halo stars. Table 1 includes the minority stars V854 Cen, V3795 Sgr, VZ Sgr and V CrA.

The mean R – the quantity R_{av} from Table 2 – is taken as a RCB’s propensity to shed puffs. The C abundances – see above remarks on the carbon problem – span a small range including both majority and minority RCBs and are uncorrelated with the mean R . The O abundances exhibit a

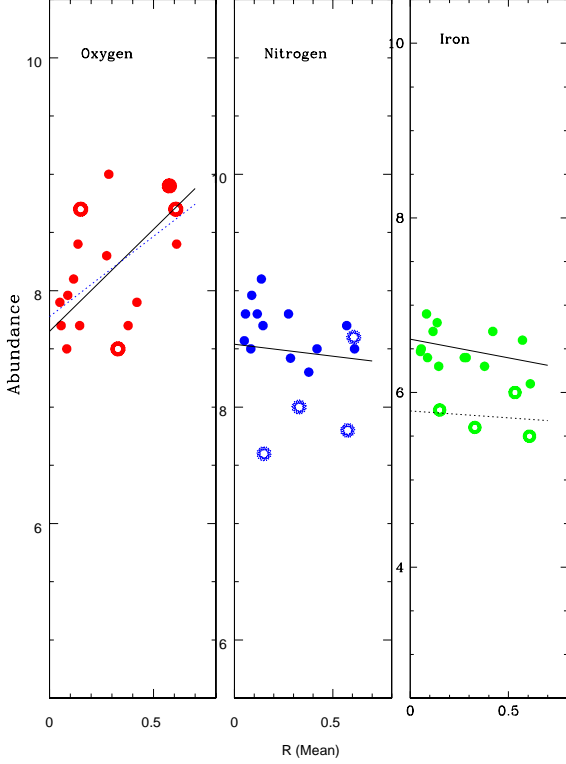


Figure 13. Abundance of photospheric oxygen (red symbols), nitrogen (blue symbols) and iron (green symbols) are plotted with respect to the mean R from Table 2. Majority RCBs are represented by filled circles and minority RCBs by open circles.

range of about 1.5 dex. There appears to be a positive correlation between the O abundance and the mean R (Figure 13) with barely a separation between majority and minority RCBs. The N abundances of majority RCB show a weak anti-correlation with the mean R with three of the four minority RCBs having a far lower N abundance (Figure 13). Similarly, the Fe abundances of the majority are weakly anti-correlated with the mean R with, of course, the Fe abundances of minority RCBs falling below those of the majority RCBs. A least squares solution of all the stars (both majority and minority) for O abundance with respect to the mean R suggests a slope of 1.24 ± 0.4 and a correlation coefficient of 0.52 which would increase to 1.33 ± 0.33 and a correlation coefficient of 0.70 if two outliers are dropped. For the N abundance with respect to the mean R , the slope is -0.5 ± 0.4 with a correlation coefficient of -0.3. For Fe abundance the majority RCBs suggest a slope of -0.4 ± 0.3 with a correlation coefficient of -0.37. For minority RCBs the Fe abundances give the slope is -0.15 ± 0.7 with a correlation coefficient of -0.14.

Correlations between abundance ratios and the mean R have also been looked for. Using the spectroscopic C abundance, the O/C ratio also shows a weak correlation with mean R without a distinction between majority and minority RCBs. A least-squares solution of the majority RCBs shows a slope of 1.54 and a correlation coefficient of 0.65. The slope becomes 1.24 ± 0.4 and correlation coefficient of 0.5 when majority and minority RCBs are considered to-

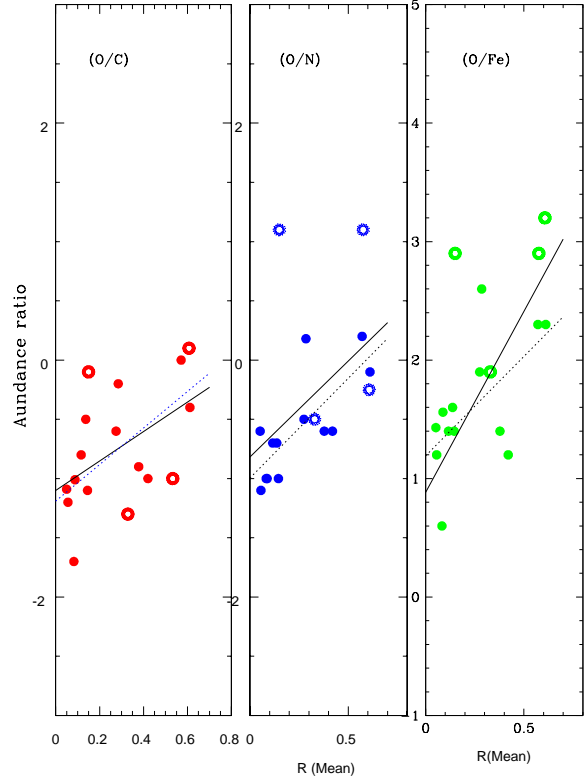


Figure 14. Photospheric abundance ratio O/C (left panel), O/N (central panel) and O/Fe (right panel) for majority (filled circles) and minority (open circles) RCBs. The solid line is the least squares fit to all stars and the dotted line is the fit for majority RCBs alone.

gether. The O/N and O/Fe ratios (Figure 14) show a rough tendency to increase with increasing mean R with two of the four minority RCBs falling amongst the majority RCBs; the exceptions among minority RCBs are VZ Sgr and V854 Cen with O/N and O/Fe ratios greater than those held by any majority RCB. The least-squares solution for O/N shows a slope of 1.7 ± 0.4 and correlation coefficient of 0.77 for majority and 0.55 for combined sample with the same slope. The O/Fe also suggests a slope of 1.67 ± 0.67 and a correlation coefficient of 0.60 for majority and combined sample has a slope of 2.17 ± 0.7 . All three abundance ratios O/C, O/N, and O/Fe seem to show a positive slope with respect mean R .

Thus, it is possible that O abundance might have an influence in dust production in these stars. Woitke et al.'s (1996) models for dust formation in RCBs suggest that the CO molecule is the most dominant cooling agent which determines whether the gas can reach condensation temperatures or not after passage of a pulsation shock. As long as the C abundance exceeds the O abundance, the CO abundance is likely to be influenced by the O abundance. It is not quite clear how the CO abundance in these stars is controlled by oxygen abundance.

3.5 Dust and Luminosity

Is dust formation related to a star's luminosity? In the absence of traditional (i.e., trigonometric) methods of estimating luminosity, we rely on the pulsation-period relation for RCBs. Pulsation is also of direct interest to the puzzle of dust formation in that a link, first suggested by Pugach (1977) and confirmed by Crause et al. (2007) ties onset of dust formation to a preferred phase in a RCBs radial pulsation. However, copious dust formation appears not to occur at every passage through the preferred phase. Also, it is unclear how dust formation is physically related to this phase. Although Woitke et al. (1996) developed a model for a shock-induced dust formation in a pulsating RCB, many details are still to be worked out, particularly in applying it to specific stars (however see Rao & Lambert 2010).

On the theoretical front, radial pulsations obey the relation $P\rho^{1/2} = Q$ where P is the period, ρ the density and Q is a constant. Following Fadeyev (1996), P in days can be written as follows

$$P = \left(\frac{T_{\text{eff}\odot}}{T_{\text{eff}}} \right)^3 \left(\frac{L}{L_{\odot}} \right)^{3/4} \left(\frac{M}{M_{\odot}} \right)^{-1/2} Q \quad (1)$$

where L and M are luminosity and mass, respectively.
1414,1 98

Pulsation periods for many RCBs have been estimated from optical photometry with measurements available in the literature for the majority of stars in Table 1 (see Table 3 and Lawson & Kilkenny 1996). Photometric amplitudes are small in most cases: less than several hundredths of a magnitude except for RY Sgr and a few others. Amplitudes may be variable and P may vary too. With few exceptions, the period P is in the range 30 – 50 days. Exceptions include U Aqr with $P = 81.3$ days (Lawson et al. 1990), $P = 114$ days for NSV 11154 (our unpublished estimate), $P=120$ days for S Aps (Kilkenny & Flanagan 1983) and $P=130$ days for Z UMi (Benson et al. 1994). Periods shorter than 30 days are found among the extreme helium stars, the hydrogen-deficient carbon stars and the hot RCBs. The T_{eff} vs P plane is shown in Figure 15. This plot is similar to Lawson et al.'s (1990) figure 32. Effective temperatures for most RCBs are spectroscopic values from Asplund et al. (2000). However for the cooler RCBs, except for Z UMi, no spectroscopic T_{eff} s are available and T_{eff} estimates are based on SED fits and photometry. Using Fadeyev's formula, we find most of the RCB stars are distributed around the locus $\log L/M = 4.0$ for M of $0.7 M_{\odot}$ with the HdC stars located around $\log L/M = 3.5$.

Within the large sample with P between 30 and 50 days, there is no correlation between the mean R and P or T_{eff} . Outside this period range, there are too few RCBs to search for connections with the mean R . However as seen from Table 2, generally cooler RCBs (presumably with longer periods) have larger mean R values. At periods shorter than about 20 days, dust formation either does not occur or is an infrequent occurrence. As noted above, the stars in this category are the EHes warmer than RCBs, the HdC stars at the cool end and the hot RCBs at the hot end of the range for RCBs. Only one HdC star that showed mild infrared excess, V4512 Sgr, is marked in Figure 15.

Better estimates of both periods as well as the mode

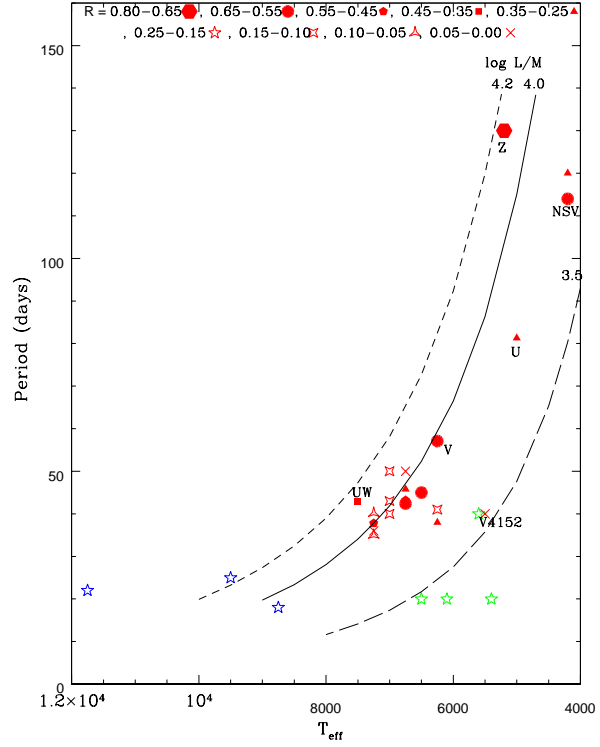


Figure 15. Effective temperature T_{eff} versus pulsation period P for RCBs (red symbols), cool EHes (blue symbols) and HdCs (green symbols). Loci of constant $\log L/M$ are shown for values of 4.2, 4.0 and 3.5 where L is the stellar luminosity and M is the stellar mass. The key for the mean R values is shown on top. Larger mean R is represented with a larger symbol. The only HdC star with IR excess, V4512 Sgr (HD175893) is shown with a red cross.

of pulsation, particularly for cool RCBs, are required for a proper assessment of the pulsation- dust connection.

3.6 Dust Mass

It might be relevant to estimate the mass of dust that is hanging around these stars. The basic relation is

$$M_d = \left(\frac{F_{\lambda}}{\kappa_{\lambda}} \right) \left(\frac{D^2}{B_{\lambda}(T_d)} \right) \quad (2)$$

where M_d is the dust mass, F_{λ} is the excess flux over the stellar flux, κ_{λ} is the absorption coefficient of the grain in $\text{cm}^2\text{gm}^{-1}$, D is the distance to the object and $B_{\lambda}(T_d)$ is the Planck function.

This quantity also depends on the estimate of the distance to the object. We use the M_v vs (V-I) colour established for LMC RCBs by Tisserand et al. (2009). As typical for F type stars UV Cas and Y Mus, we assume the M_v to be -5 and estimate the distance. Also assuming the dust to be amorphous carbon of BE type (Colangeli et al. 1995) we estimate the dust mass at the time of IRAS observations as $2.9 \times 10^{-9} M_{\odot}$ for both UV Cas and Y Mus. A similar estimate for cool RCB Z UMi is obtained, by assuming M_v of -3.5 as consistent with the observed V-I colour, as $4.8 \times 10^{-9} M_{\odot}$ at the time of IRAS observations.

Table 3. Pulsations and dust

Star	T_{eff} K	Period days	R(mean)	Period Ref.	Comment
UW Cen	7500	42.79	0.38	Crause et al (2007)	
Y Mus	7250	35.0	0.06	Marang et al (1990)	
XX Cam	7250	36	0.01	Weiss et al (1996)	
RY Sgr	7250	37.79	0.42	Crause et al (2007)	
UV Cas	7250	40.16	0.08	Weiss et al (1996)	
RT Nor	7000	43	0.14	Lawson et al (1990)	
VZ Sgr	7000	40 ^a	0.15	Lawson & Cottrell (1997)	
UX Ant	7000	50	0.14	Lawson et al (1994)	
RS Tel	6750	45.8	0.28	Lawson et al (1990)	
RZ Nor	6750	42.4 ^b	0.57	Lawson et al (1990)	
R CrB	6750	42.7 ^c	0.28	Rao et al (1999)	
V854 Cen	6750	43.25	0.58	Crause et al (2007)	
V532 Oph	6750	50	0.05	Clayton et al (2009)	
SU Tau	6500	45.07	0.61	Weiss et al (1996)	
V CrA	6500	57.1	0.61	Lawson et al (1990)	
FH Sct	6250	41	0.14	this paper	
U Aqr	5000	81.3	0.31	Lawson et al (1990)	
Z UMi	5200	130	0.74	Benson et al (1994)	
S Aps	4200	120 ^d	0.29	Kilkenny & Flanagan (1983)	
NSV11154	4200	114 ^f	0.65	unpublished	
FQ Aqr	8750	18		Kilkenny et al (1999)	coolEHe
LSIV-14 109	9500	25		Lawson et al (1993)	coolEHe
NO Ser	11750	22		Kilkenny et al (1999)	coolEHe
V2244 Oph	12750	10		Lawson et al (1993)	coolEHe
HD175893	5500	41.0	0.026	Lawson et al (1990)	HdC
HD137613	5400 ^e	20		Kilkenny et al (1988)	HdC
HD148839	6500	20		Kilkenny et al (1988)	HdC
HD182040	5600	40		Kilkenny et al (1988)	HdC
HD173409	6100	20		Kilkenny et al (1988)	HdC

^a - 47days according to Bateson (1978)^b - 68 days?^c - Photometric period changes 43-53 days according to Fernie & Lawson (1993), Lawson & Kilkenny (1997) and Percy et al (2005). We use the period determined from radial velocities obtained over several decades (Rao et al. 1999) .^d - see the discussion in Lawson et al (1990).The period changes occur. The period quoted here might be a fundamental mode as detected by Waters (1966) and Kilkenny & Flanagan (1983).^e - Kipper (2002) gives T_{eff} of 6000 K and $\log g$ of 1.3 for HD137613 (= HM Lib).^f - Period is variable. The mean period may be 114 days.

Clayton et al. (2011) imaged R CrB and its environment during the prolonged deep minimum that started in 2007. They discovered several cometary knots around the star which are interpreted as past ejected dust puffs from the star. As they state ‘The puffs cause declines when they form directly in our line of sight and may be seen as cometary knots when they form to the side of or behind R CrB’. It is interesting to note that the dust mass estimated for these knots of $10^{-8} m_{\odot}$ to $10^{-9} m_{\odot}$ is about equal to dust mass estimated above for UV Cas, Y Mus and Z UMi from midIR excess at any given instant. It is of interest to note that Clayton et al. (2011) estimate total dust mass of $10^{-2} m_{\odot}$ for the R CrB shell including the cold dust from their observations into far infrared with *Herschel*.

4 CONCLUDING REMARKS

Variations in the mid-IR flux densities measured by the different satellites reflect changes in the circumstellar shell’s mid-IR emission. Plots comparing flux densities from the four IR satellites are provided in Figures 1, 2 and 3. It is of

interest to tease from such comparisons the intrinsic changes in mid-IR emission. Identification of intrinsic changes is certainly secure for the extreme outliers in the figures – most notably, UV Cas (Figure 4), S Aps (Figure 5) and RT Nor (Figure 6). These must arise from the varying contribution of puffs in the circumstellar shell; the scale of these variations far exceeds the measurement uncertainties. As discussed above, UV Cas’s high *IRAS* flux densities arise from puffs emitted somewhat prior to the *IRAS* observation and, as these puffs evolved away from the star and cooled, lower flux densities were measured by the later satellites and in the ground-based important series of measurements by Bogdanov et al. (2010). Somewhat similarly, RT Nor owes its position as an outlier to the appearance of fresh puffs between the *Spitzer* and *WISE* observations and some fraction of these puffs caused the deep optical decline recorded by *AAVSO* observers.

Extreme outliers are valuable because they provide a measure of the contribution to the mid-IR emission from an individual puff or a collection of associated puffs; RT Nor experiences a 0.4 increase in R between the *Spitzer* and *WISE*

observations. Other RCBs with a circumstellar shell occupied by several to many puffs will experience smaller variations in their mid-IR emission. One might suppose that variations will decrease in size as the number of puffs increases.

Stars where the mid-IR emission appears to be dominated by the slow evolution of the circumstellar dust offer the opportunity to test theoretical ideas. In particular, movement of a given family of puffs away from the star is predicted to lead to the relation $R \propto T_d^4$. As shown in Section 3.3 and, in particular by Figure 12, this prediction is well verified by stars where the mid-IR emission is thought to come from a single collection of puffs. In other cases, the observations scatter about the predicted relation in a plausible fashion.

Puff creation aside, evolution of the mid-IR emission from existing puffs is anticipated to be a slow process, as revealed by the case of UV Cas. Equilibrium temperatures of a gray grain (see Paper I and above) about a typical RCB are predicted to run from about 1300K at 10 stellar radii to 500K at 50 stellar radii to 250K at 200 stellar radii. If the dust grains are repelled from the star at about 10 km s⁻¹, their path from their formation at (say) 10 stellar radii to about 200 stellar radii will take about 40 years. Thus, over the duration spanned by *AKARI*, *Spitzer* and *WISE*, the mid-IR emission from a given set of puffs will evolve very little, except for the formation of fresh puffs. Optical depth effects at visible and infrared wavelengths may complicate this simple expectation. Extending the time span to include *IRAS* should reveal a steady evolution, as indeed is shown in Figure 12. Toward the end of a deep decline, a high-velocity wind is seen as a blue-shifted absorption component to the Na D and other strong resonance lines: radial velocities attain about 200 km s⁻¹ (Rao et al. 1999). This wind's origin is unknown but, if it can sweep outward gas and dust ahead to it, it offers an explanation for some examples (e.g., V3795 Sgr) of evolution of mid-IR emission much more rapid than observed for UV Cas and similar cases. Of course, this high-speed wind can affect the mid-IR emission along any radius vector where puffs have accumulated. Evolutionary timescales for RCBs are several hundreds of years at least. One may suppose that a RCB's propensity to form and eject dusty puffs evolves during this time. Some interesting insight that emerged from these midIR studies of RCBs are that the oxygen abundance has some influence on the dust production. It also appears that cool RCBs have more dust around them and higher luminosity at a given mass helps in dust production. Studies of pulsations, particularly in cool RCBs, would be a great help in future understanding of dust production in these stars.

Observational insights into the formation and evolution of dust around RCB stars are limited by the paucity of measurement at IR wavelengths. Campaigns extending Bogdanov et al.'s (2010) close scrutiny of UV Cas to other RCBs are to be encouraged. Such a campaign should extend to long wavelengths the valuable two decade long programme of *JHK*L photometry of a dozen southern RCBs by Feast et al. (1997; see also Feast 1997). Although, as shown here, the four IR satellites from *IRAS* to *WISE* have provided valuable insights into the evolution of circumstellar dust for a major sample of RCBs, it is most unlikely that a satellite

will ever provide a thorough collection of IR photometry of these rare and fascinating stars.

5 ACKNOWLEDGEMENTS

We appreciate various comments made by the referee Geoff Clayton which improved the paper a great deal. We thank Anibal García-Hernández for his assistance with the preparation and analysis of the observations of RCBs with the *Spitzer* satellite. We acknowledge with thanks the variable star observations from the AAVSO database. This research has made use of the SIMBAD database, operated at CDS, Strasbourg, France. This research has been supported in part by the grant F-634 from the Robert A. Welch Foundation of Houston, Texas.

REFERENCES

- Asplund, M., Gustafsson, B., Kiselman, D., Eriksson, K. 1997, *A&A*, 323, 286
- Asplund, M., Gustafsson, B., Rao, N. K., Lambert, D.L. 1998, *A&A*, 332, 651
- Asplund, M., Gustafsson, B., Lambert, D.L., Rao, N.L. 2000, *A&A*, 353, 287
- Bateson, F.M. 1978, *Publ. Var. Star Sec. R. Astr. Soc. New Zealand*, 6, 39
- Benson, P.J., Clayton, G.C., Garnavich, P., Szkody, P. 1994, *AJ*, 108, 247
- Bogdanov, M.B., Taranova, O.G., Shenavrin, V.I. 2010, *Astr. Rep.*, 54, 620
- Chesneau, O., Millour, F., De Marco, O., Bright, S.N., Spang, A., Lagadec, E., Mékarnia, D., de Wit, W. J. 2014, *A&A*, 569, L4
- Clayton, G.C., 2012, *JAAVSO*, 40, 539
- Clayton, G.C., Geballe, T.R., Zhang, W., 2013, *AJ*, 146, 23
- Clayton, G.C., Bjorkman, K.S., Nordsieck, K.H., Zellner, N.E.B., Schulte-Ladbeck, R.E., 1997, *ApJ*, 476, 870
- Clayton, G.C., Whitney, B.A., Stanford, S.A., Drilling, J.S., 1992, *ApJ*, 397, 652
- Clayton, G.C., Kilkenny, D., Wils, P., Welch, D.L., 2009, *PASP*, 121, 461
- Clayton, G.C et al., 2011, *ApJ*, 743, 44
- Colangeli, L., Mennella, V., Palumbo, P., Rotundi, A., Bussoletti, E., 1995, *A&AS*, 113, 561
- Crause, L.A., Lawson, W.A., Henden, A.A., 2007, *MNRAS*, 375, 301,
- Fadeyev, Yu. A., 1996, in: *Hydrogen deficient stars*, Jeffery C.S., Heber U. (eds.). ASP conf. series vol. 96, p. 375
- Feast, M.W., 1979, in: *Changing Trends in Variable star research*, Bateson, F.M, Smak, J., Urch, I.M. (eds.), Univ. of Waikato, Hamilton, N.Z., IAU. Coll. 46, p 246
- Feast, M.W., 1986, in: *Hydrogen deficient stars and Related Objects*, Hunger, K., Schönberner, D., Kameswara Rao, N (eds.). Reidel, Dordrecht) p 151
- Feast, M.W., 1996, in: *Hydrogen deficient stars*, Jeffery C.S., Heber U. (eds.). ASP conf. series vol. 96, p. 3
- Feast, M.W., 1997, *MNRAS*, 285, 339
- Feast, M.W., Glass, I., 1973, *MNRAS*, 161, 293
- Feast, M.W., Carter, B.S., Roberts, G., Marang, F., Catchpole, R.M. 1997, *MNRAS*, 285, 317
- Fernie, J.D., Lawson, W.A., 1993, *MNRAS*, 265, 899
- García-Hernández, D.A., Kameswara Rao, N., Lambert, D.L., 2011, *ApJ*, 739, 37 (paper I)
- García-Hernández, D.A., Kameswara Rao, N., Lambert, D.L., 2013, *ApJ*, 773, 107 (paper II)

Glass, I.S., 1978, MNRAS, 185, 23

Goldsmith, M.J., Evans, A., Albinson, J.S., Bode, M.F., 1990, MNRAS, 245, 119

Herbig, G.H., 1949, ApJ, 110, 143

Iben, I., Jr. 1991, ApJS, 76, 55

Ishihara, D. et al. 2010., A& A, 514, 1

Jurcsik, J., 1996, AcA, 46, 325

Kilkenny, D., Flanagan, C., 1983, MNRAS, 203, 19

Kilkenny, D., Whittet, D.C.B., 1984, MNRAS, 208, 25

Kilkenny, D., Marang, F., Menzies, J.W., 1988, MNRAS, 233, 209

Kilkenny, D., et al., 1999, MNRAS, 305, 103

Kipper, T., 2002, Bal.Astr., 11, 249

Kwok, S. 2007, Physics and Chemistry of the Interstellar Medium, (Sausalito: Univ. ScienceBooks)

Lambert, D. L., Rao, N. K., 1994, JAA, 15, 47

Lambert, D.L., Rao., N.K., Pandey., G., Ivans, I., 2001, Ap.J., 555, 925

Lawson, W. A., Cottrell, P.L. 1997, MNRAS, 285, 266

Lawson, W. A., Cottrell, P. L., Kilmartin, P.M., Gilmore, A.C., 1990, MNRAS, 247, 91

Lawson, W. A., et al., 1993, MNRAS, 265, 351

Lawson, W. A., Cottrell, P. L., Clark, M., 1991, MNRAS, 251, 687

Lawson, W.A., Kilkenny, D., 1996, in: Hydrogen deficient stars, Jeffery C.S., Heber U. (eds.). ASP conf. series vol. 96, p. 349

Lawson, W. A., et. al., 1994, MNRAS, 271, 919

Loreta, E., 1934, AN., 254, 151

Marang, F., Kilkenny, D., Menzies, J.W., Jones, J.H. Spencer., 1990, SAAOC, 14, 1

Miller et al. 2012, ApJ, 755, 98

O'Keefe, J.A., 1939, ApJ, 90, 294

Payne-Gaposchkin, C., 1963, ApJ, 138, 320

Percy, J.R., Bandara, K., Cottrell, P. L., Skuljan, L. 2004, JAVSO, 33, 27

Pugach, 1977, IBVS 1277

Rao, N.K., Nandy, K., 1986, MNRAS, 222, 357;

Rao, N.K., Lambert D.L., 1993, AJ, 105, 1915

Rao, N.K., Lambert D.L., 2003, PASP, 115, 1304

Rao, N.K., Lambert D.L., 2010, in: Recent Advances in Spectroscopy, Chaudhuri, R.K., Mekaden, M.V., Raveendran, A.V., Narayanan, A.S. (eds). ASSP:Springer, p 177

Rao, N.K., Lambert D.L., Adams, M.T., Doss, D.R., Gonzalez, G., Hatzes, A.P., James, R., Johns-Krull, C.M., Luck, R.E., Pandey, G., Reinsch, K., Tomkin, J., Woolf, V.M. 1999, MNRAS, 310, 717

Rao, N.K., Lambert, D.L., Woolf, V., Hema, B.P., 2014, PASP, 126, 813

Tisserand, P., 2012, A&A, 539, 51

Tisserand, P., et al., 2009, A& A, 501, 985

Tisserand, P., et al., 2011, A& A, 529, 118

Tisserand, P., et al., 2013, A& A, 551, 77

Walker, H., 1986, in: Hydrogen deficient stars and Related Objects, Hunger, K., Schonberger, D., Kameswara Rao, N (eds.). Reidel, Dordrecht, p 407

Waters, B.H.J., 1966, R. astr. soc. N. Zealand Circulars, 119

Weiss, A., Fried, R., Olson, E.C., 1996, A& AS, 116, 31

Woitke, P., Goeres, A., Sedlmayr, E., 1996, A& A, 313, 217

Wright, E.L., et al., 2010, A.J., 140, 1868